Chemical reactions in restricted spaces: Decay in the presence of quenchers

P. Lianos
University of Patras, School of Engineering, 26 000 Patras, Greece

P. Argyrakis
Department of Physics 313-1, University of Thessaloniki, 54 006 Thessaloniki, Greece
(Received 25 August 1988)

We have fitted computer simulation data for the $A+B\rightarrow 0$ reaction (where $[A]<[B]$) to a kinetic scheme based on the decay equation $[A]=[A]_0\exp(k_1Qt^{2g}-k_2Qt^g)$ previously utilized in luminescence quenching in microemulsion droplets [P. Lianos, J. Chem. Phys. **89**, 5237 (1988)]. We used a percolation model of clusters below the critical threshold with a specified range in cluster size. The $[A]/[B]$ density ratio was either constant or varying as a function of p (p is the probability for an allowed site). Our conclusions show that the resulting spectral dimension of the reaction process is always smaller numerically than the customary value $d_s=\frac{4}{3}$, and that it is strongly dependent on the size and shape of the reaction space. Relevant experiments where these situations arise are also discussed.

I. INTRODUCTION

An increasing interest has been shown recently in describing inhomogeneous systems as fractal objects. Fractal modeling has been successfully applied to transport and interactions in solid-state physics but recent findings[1-4] indicate that it may as well be useful in describing interactions in such microheterogeneous systems as microemulsions. Furthermore, it seems that the kinetics of reactions between highly compartmentalized reactants can be expressed in terms of the fractal and spectral (noninteger) dimension of the reaction medium. This situation arises in many experimental situations. Consider an excited luminescent molecule, say L^*, that is solubilized within, for example, micelles not allowing exchange of solubilizates between them. This work shows that in the presence of quenchers Q at higher concentration than L^* the luminescence decay obeys the equation[2]

$$I=I_0\exp(-k_0t)\exp(+k_1Qt^{2g}-k_2Qt^g)\ , \qquad (1)$$

where k_0 is the luminescence decay rate constant in the absence of quenching, k_1 and k_2 are constants, Q is the quencher concentration, and g is a positive number smaller than unity. The same equation should apply for any reaction $A+B\Longrightarrow$ products, where the concentration $[A]$ is substantially smaller than the concentration $[B]$. If $[A]$ is monitored by some other means than luminescence then Eq. (1) should be used without the factor $\exp(-k_0t)$. The term k_2Qt^g is exact, but the term k_1Qt^{2g} is an approximation of a series with an infinite number of terms.[2,3,5] A similar equation has been successfully applied to describe multistep energy transfer, where g equals one-half of the spectral dimension.[4,6] The verification of Eq. (1) has been done by fitting it to experimental decay profiles of luminescent molecules solubilized in water-in-oil microemulsions or phospholipid vesicles.[2,3] To test the validity of this model with a different approach we resort in the present work to equivalent reactions simulated by Monte Carlo methods.

Recently[7] considerable effort has been made to elucidate the kinetics of reactions of the $A+A$ and $A+B$ type for inhomogeneous spaces, such as fractals, surfaces, lines, porous materials, membranes, etc. The major conclusion of these works is that the kinetics in these spaces is highly nonclassical and the rate laws are dominated by the so-called spectral dimension. However, for the $A+B$ reaction only the $[A]=[B]$ simpler case has been studied, and practically all effort has been placed in understanding the segregation of reactants that takes place in this type of reaction. In the present work $[A]$ is much smaller than $[B]$. The reason for this choice is found in numerous works of luminescence probing of organized molecular assemblies.[8] In the present computer simulation procedures the reaction medium has been chosen to be the clusters formed by a two-dimensional binary lattice which has a concentration p of open (allowed) sites less than p_c, the critical percolation threshold. Even though most of the work on reactions up to now is done exactly at the critical threshold we choose here to utilize clusters of small sizes and avoid the infinite cluster at p_c. This is because real organized assemblies,[8] such as micelles,[8] microemulsion droplets,[2] vesicles,[3] etc., have a lower size limit of the order of a few tens of angstroms. Thus we use as a lower limit of cluster size $s=25$ sites. As far as the upper limit is concerned we arbitrarily choose $s=50$, 250, and ∞, since the above systems are also found in a great variety of sizes. Thus we restrict all reactions within these bounds in our effort towards understanding the luminescence mechanisms of several experimental systems. In Sec. II we describe the techniques that we used for the computer simulations. In Sec. III we present our results, and finally in Sec. IV our conclusions.

II. COMPUTATIONAL METHODS

The computer simulation of the chemical reactions was done using the techniques previously reported.[9] Briefly, the lattice clusters are generated on a 300×300 square lattice at a given p, the probability for an open site. As stated above a minimum and maximum cluster size are also specified, and only the clusters that fall within this prescribed s range are kept, while all the rest become nonaccessible sites. A certain number of A and B particles are placed at random on the available clusters at time $t=0$. Reaction proceeds in the known way, i.e., all particles perform random walks with the stipulation that when an A and B particle occupy the same site they annihilate and are removed from the system, while nothing happens between two A or two B particles. We use excluded volume principles, i.e., we do not allow more than one particle to occupy a given site at any one time. We monitor the density of A particles $[A]$ as a function of time. The basis for our time unit is one Monte Carlo step (MCS), which is defined as the time it takes for all present particles to move one step to one of their nearest neighbors. In these calculations times goes from 0 to 200 MCS. This may correspond to a realistic situation when 1 MCS=1 nsec. For example, in pyrene excimer probing of micelles formed with tetradecyltrimethylammonium halides[10] the monomer decay time ranges between 160 and 300 nsec. We monitored several interactions with several $[A]/[B]$ ratios. We noticed that when this ratio is less than 0.20 the reaction proceeds too fast to allow appropriate analysis, as the number of A reactants is too small. Subsequently, we carried out all calculations by using a ratio $[A]/[B]=0.20$. In real luminescence quenching experiments the $[L^*]/[Q]$ ratios are substantially smaller, but this does not change the conclusions of this work. Our choice of the $[A]/[B]$ ratio is dictated here by the available number of lattice sites, and using a larger lattice could easily accommodate for different ratios, albeit more time consuming.

We distinguish two cases: (i) $[A]$ is constant for all p values. This means that the absolute number of A particles (and B) varies with the total number of the available reaction sites as p varies. (ii) The total number of A (and B particles) remains constant, independently of p. This means that $[A]$ is not constant with p.

III. RESULTS AND DISCUSSION

We start with case (i). Equation (1) was fitted to all annihilation decay curves by nonlinear regression, least-square analysis. We monitored reactions at clusters generated at several different p values in the range $p=0.34$–0.58. The fit was very good, as seen in the example of Fig. 1. It was equally good for both this case and the second case presented below. This is a sound verification of the validity of this equation. Fitting gave the values of the corresponding parameters. The fitted equation was in fact written as

$$[A]=[A]_0\exp(+C_1t^{2g}-C_2t^{g}) , \tag{2}$$

where $C_1=k_1Q$ and $C_2=k_2Q$. Notice that the factor $\exp(-k_0t)$ of Eq. (1) does not come into Eq. (2), since $[A]$ is not monitored by luminescence. The time dependence of $[A]$ in Eq. (2) always has an exponentially decaying form since it is always true that $C_2t^{g}>C_1t^{2g}$. This is because the term C_2t^{g} is the leading term, while the term C_1t^{2g} (and more such terms) have geometrically decreas-

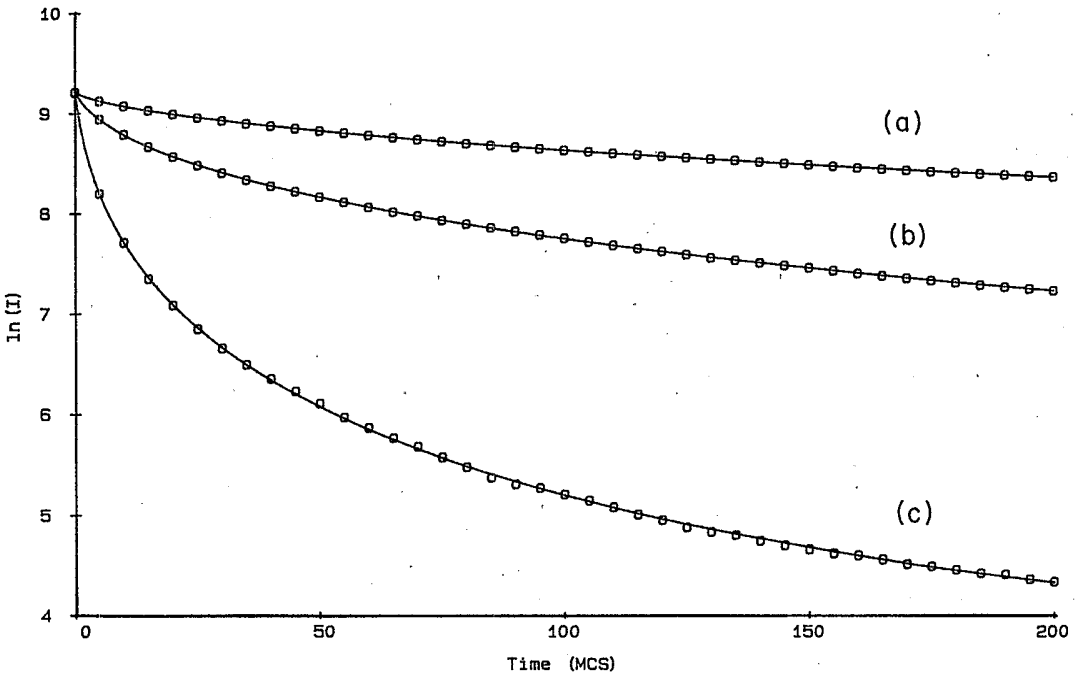

FIG. 1. Decay of the $[A]$ density for the $A+B\Longrightarrow0$ reaction. Solid lines are solutions of Eq. (2). Circles are results from the computer simulated reactions at $p=0.58$. Three different cluster size ranges are given: (a) $25<s<\infty$, (b) $25<s<250$, and (c) $25<s<50$.

ing values [see, for example, Eq. (13) of Ref. 11, where $C_1 \sim \lambda^2$, $C_2 \sim \lambda$, and $\lambda \ll 1$]. The measured values of the parameter g are shown in Table I. We observe that g varies substantially with p between about 0.44 to 0.57. The variation of the power of time creates a problem as far as the units of C_1 and C_2 are concerned. Therefore, in order to get a realistic picture of the values of the constants C_1 and C_2 and to follow their behavior, we have reduced C_1 and C_2 to C_{1r} and C_{2r}, respectively, by raising each value to a power necessary to reduce the corresponding values of g to 1. The obtained C_{2r} values are also shown in Table I. Notice that as p increases from 0.34 to 0.58 the C_{2r} values show a substantial variation. Similarly with C_{1r} (not shown) which, however, were calculated with a considerable uncertainty. This is most probably due to the fact that the exact Eq. (1) contains an infinite number of terms, while its present form is only an approximation, as mentioned above.

TABLE I. g, C_{2r}, and reduced C_{2r}/N values for case I of text.

p	g	$10^7 C_{2r}$	$10^3 C_{2r}/N$
	Cluster size $25 < s < \infty$		
0.34	0.54	4.9	58.8
0.37	0.50	5.6	25.1
0.40	0.44	6.1	12.5
0.45	0.48	6.2	4.8
0.47	0.48	6.1	3.5
0.48	0.45	6.7	3.1
0.49	0.47	6.2	3.1
0.50	0.47	6.2	2.5
0.55	0.45	7.3	2.0
0.57	0.50	6.8	1.6
0.58	0.49	6.7	1.5
	Cluster size $25 < s < 250$		
0.34	0.57	4.7	56.0
0.37	0.46	6.0	27.0
0.40	0.45	5.8	11.9
0.45	0.48	5.9	4.5
0.47	0.48	6.3	3.6
0.48	0.47	6.3	3.2
0.49	0.47	6.4	3.0
0.50	0.48	7.0	3.0
0.55	0.48	6.6	3.3
0.57	0.49	6.9	5.2
0.58	0.49	7.0	7.0
	Cluster size $25 < s < 50$		
0.34	0.57	4.7	57.5
0.37	0.46	6.1	29.7
0.40	0.45	5.8	14.1
0.45	0.48	5.9	7.3
0.47	0.45	6.5	7.4
0.48	0.48	6.4	7.2
0.49	0.45	6.5	7.5
0.50	0.48	6.4	7.6
0.55	0.49	6.6	13.6
0.57	0.50	6.7	20.0
0.58	0.52	6.6	24.6

Figures 2 and 3 give information necessary to analyze the above data. In Fig. 2 we plot the average cluster sizes I_{av} versus p for the three different ranges that we used. I_{av} is calculated in the standard method as the second moment of the cluster distribution.[12] The proper equation that was used is the following:

$$I_{av} = \sum_{s_{min}}^{s_{max}} i_s s^2 \Big/ \sum_{s_{min}}^{s_{max}} i_s s \ , \tag{3}$$

where s is the cluster size and i_s is the frequency of its appearance. The lower and upper limits in these sums are the limits of our size ranges. In Fig. 2 we see that the average cluster size I_{av} increases as p increases, as expected. At large p the clusters become larger and less numerous. At $p=0.58$, i.e., close to the percolation threshold, practically only one cluster of very large size is about to be formed. As we expect $s \Longrightarrow \infty$ when p approaches the percolation threshold. The variation, however, of the average number of sites N on which reaction can occur is not monotonous. In Fig. 3 we plot this number N versus p. We observe here that the case $25 < s < \infty$ behaves as expected for cluster sizes without an upper limit. The other two cases show a maximum since the cutoff of large size clusters at high p excludes an increasing number of reaction sites. Thus, by properly choosing the limits in the values of s we have a model in which we directly control the size and shape of the reaction medium and can later apply it to specific experimental systems.

The data of Figs. 2 and 3 together with Table I allow for some interesting conclusions. The value of C_{2r} is equivalent to a second-order reaction rate constant multiplied by the global concentration (density) Q of the majority reactant, i.e., in our case by $[B]$. Since $[B]/N$ is constant, the global value of $[B]$ increases proportionally to the value of N. To recover then an equivalent second-order rate constant for the sake of comparison, we have divided all C_{2r} values by the corresponding N and the resulting numbers are also given as C_{2r}/N in Table I. We believe that this last column is the best representation of the reaction rates. Notice that the C_{2r}/N ratios vary as p increases. In the case of $25 < s < \infty$, C_{2r}/N decreases monotonically while in the other two size domains minima are observed. These results can be associated with the variations of N observed in Fig. 3. Thus when the number of the available sites increases the reaction rate decreases since in this case the random walker would need more steps (more time) before a reaction can occur. Notice that at small p no apparent differences are observed in the rate constants. But for higher p the size and shape of the resulting clusters dominate the behavior of the reaction rates.

Our Eq. (2) is equivalent to an equation used for energy migration in doped crystals.[6] This is natural, as the motion of reacting species follows the diffusion process of mass or energy in restricted spaces. For these systems random-walk models have been very successful in the near past. Our exponent g in Eq. (2) is proportional to the fractal dimension of the reaction medium.[2,3] Thus, in our previous works we have stated that $g = d_f/\alpha$ where

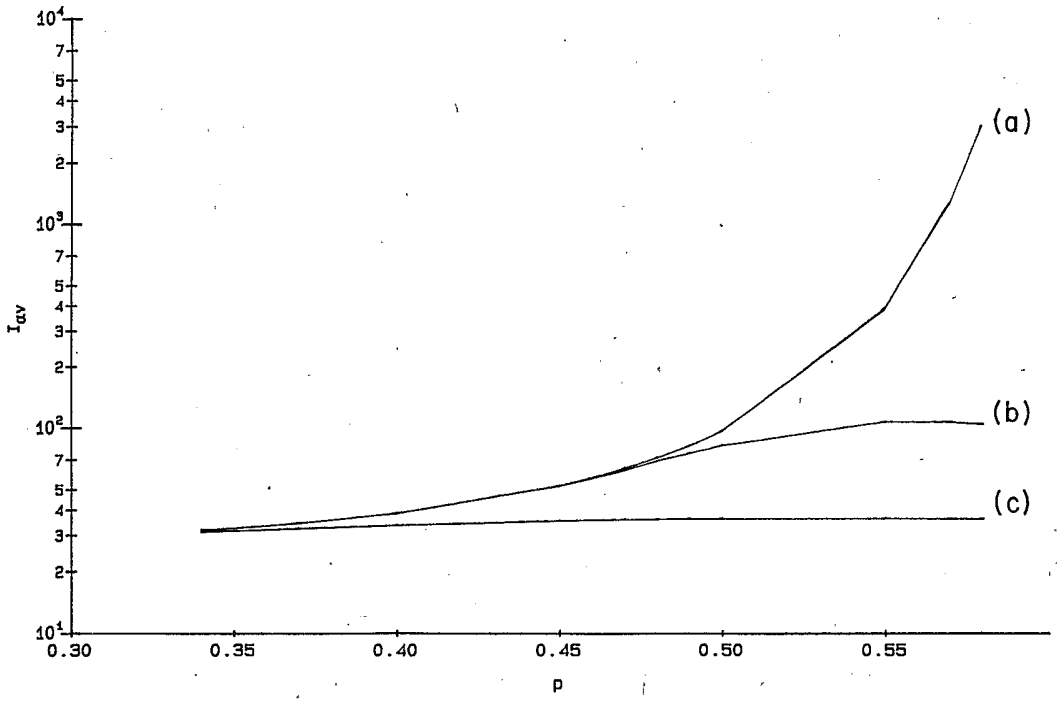

FIG. 2. I_{av} vs p for the three cluster size ranges studied. The function I_{av} is calculated using Eq. (3). The designations are the same as in Fig. 1.

$\alpha > d_f$ (d_f is the fractal dimension). α can take any positive value but it is related to the classical rate for diffusion controlled reactions,[2,3] i.e., $w \sim d_f / l^{\alpha}$, where w is the reaction rate and l is the mean diffusion path. For homogeneous spaces $\alpha = 2$. In some micelles and microemulsions we have found[2] $\alpha > 2$. These results point to the direction that $g = d_s/2$ (d_s is the spectral dimension).[4,6] In fact it has been established[13–15] that $d_s/2 = d_f/d_w$ where $d_w > 2$ in agreement to our findings that $\alpha > 2$. The quantity d_w is the fractal dimension of the path of the random walk, and it is related to the scaling of the mean-square displacement. Typical d_w values[14]

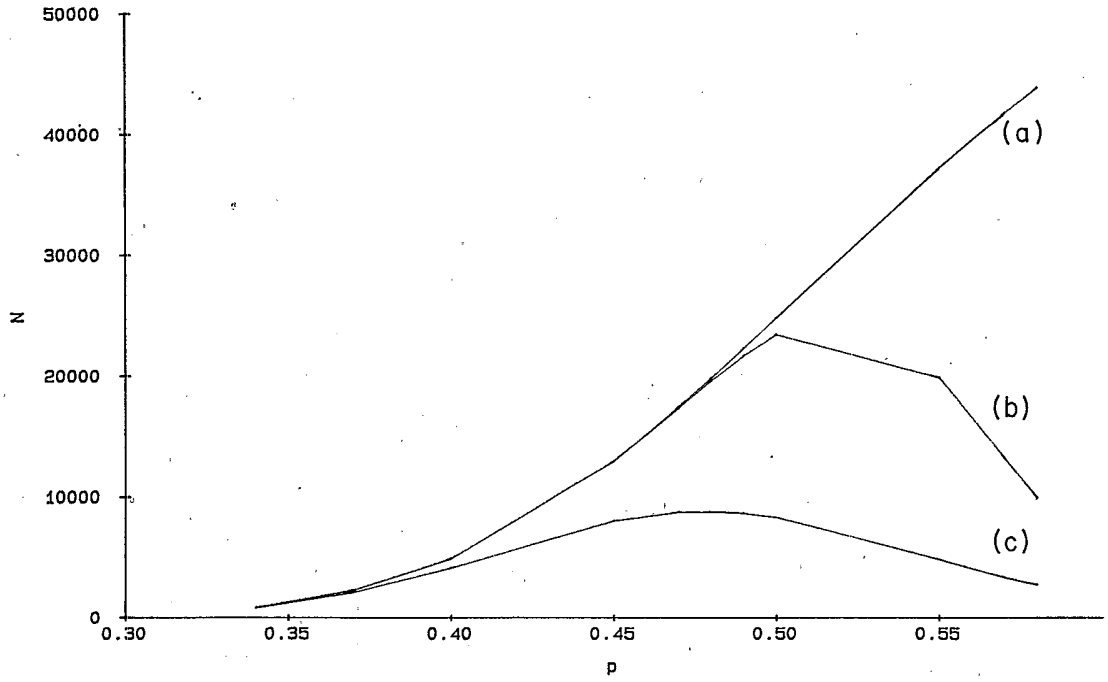

FIG. 3. N vs p for the three cluster size ranges studied. N gives the absolute number of sites on which the reaction can occur. The designations are the same as in Fig. 1.

are $d_w=2.32$ (two-dimensional Sierpinski gasket), $d_w=2.87$ (two-dimensional percolation cluster), etc. The variation then of the g values in Table I indicate a complex way with which the fractal dimension and the nature of the reactants' random walk vary with p. We notice that d_s $(=2g)$ is relatively large at small and large values of p, and it goes through a minimum in-between. Close to the percolation threshold d_s increases to approach the value of $\frac{4}{3}$ according to the Alexander-Orbach conjecture.[7,9,13,15] This value is never reached since our method is not designed for situations at the critical point, and subsequently it should not be applied there. An important finding of this work is the increase of d_s at low p which, as it will be seen below, is true only when the concentration ratio $[A]/p$ remains constant, as in the present case [case (i)]. Some small variations of g in Table I, as for example in the $p=0.34$ and 0.37 values, are attributed to statistical fluctuations.

In the second case where the total number of A and B particles remained constant, the decay profiles were again perfectly described by Eq. (2) as seen in Fig. 1. Table II gives the same information as Table I, i.e., it shows the values of g, C_{2r}, and C_{2r}/N for this case. Notice that the values of g vary with p in a very different manner than in the first case. g increases monotonically when no upper size limit is imposed on the clusters, but it shows maxima when such a restriction comes into effect. The g values in the present case follow the distribution of the total number N of the available reaction sites. When the clusters are small they are also more numerous causing an extensive separation of the reactants and making the reaction more difficult. The reaction rates are then far from the classical behavior. Subsequently g is far from unity. When the clusters increase in size and decrease in number, the situation evolves in the opposite direction. The present case is the most realistic representation of a real luminescence quenching interaction in micelles. Thus small g values are found in cases of small micelles.[16] But the relation between the present work with experimental systems needs further elaboration and it is currently under study.

Notice that in the present case g tends to a saturation value of 0.54 as p increases. This fact suggests that the model of Eq. (2) cannot describe the situation at the percolation threshold. Nevertheless values of d_s larger than $\frac{4}{3}$ have been measured in large microemulsion droplets[2] as well as in large multilamelar phospholipid vesicles.[3] The occurrence of such large values is also currently studied.

The variation of C_{2r}/N with p was essentially similar as in the first case, but differences between different size domains are more pronounced here. Apparently, the second-order reaction rates are dominated by the size of the clusters in which reaction occurs in each particular case.

TABLE II. g, C_{2r}, and reduced C_{2r}/N values for case II of text.

p	g	$10^7 C_{2r}$	C_{2r}/N
	Cluster size $25<s<\infty$		
0.37	0.236	8585.0	6.82×10^6
0.40	0.391	40.6	8.33×10^4
0.45	0.496	3.5	2.69×10^3
0.47	0.491	2.0	1.15×10^3
0.48	0.528	1.6	8.08×10^2
0.49	0.506	1.3	5.84×10^2
0.50	0.530	1.0	4.03×10^2
0.55	0.526	0.6	1.61×10^2
0.57	0.545	0.5	1.20×10^2
0.58	0.550	0.4	0.91×10^2
	Cluster size $25<s<250$		
0.37	0.225	12 065.0	5.70×10^6
0.40	0.388	41.4	8.49×10^4
0.45	0.500	3.4	2.62×10^3
0.47	0.488	2.1	1.21×10^3
0.48	0.518	1.6	8.16×10^2
0.49	0.487	1.3	6.00×10^2
0.50	0.504	1.1	4.69×10^2
0.55	0.524	1.7	8.54×10^2
0.57	0.481	3.9	2.93×10^3
0.58	0.476	7.3	7.32×10^3
	Cluster size $25<s<50$		
0.37	0.211	27 854.0	1.36×10^8
0.40	0.452	40.0	9.72×10^4
0.45	0.454	10.5	1.31×10^4
0.47	0.458	8.5	9.66×10^3
0.48	0.467	8.1	9.17×10^3
0.49	0.470	8.2	9.40×10^3
0.50	0.458	9.9	1.18×10^4
0.55	0.461	30.6	6.30×10^4
0.57	0.378	162.0	4.84×10^5
0.58	0.338	489.0	1.82×10^6

IV. CONCLUSION

The present work shows that the interaction between compartmentalized reactants A and B, where the density (concentration) of $[A]$ is substantially smaller than $[B]$, follows the kinetics of Eq. (2) where $g<1$. g is equal to d_f/α where d_f is the fractal dimension and $\alpha=d_w$. g can also be written as $d_s/2$ where d_s is the spectral dimension. The full form of Eq. (2) is necessary in order to achieve the observed agreement in Fig. 1. If $C_1=0$, no such agreement is observed, showing the importance of the $C_1 t^{2g}$ term in our system.

The values of g were calculated by fitting Eq. (2) to the decay profiles obtained by Monte Carlo simulation of the reaction between A and B in isolated clusters formed in a binary lattice. The g values give the spectral dimension of the reaction space. Thus the spectral dimensions were always smaller than $\frac{4}{3}$, the typical value for the percolation threshold. They were strongly dependent on the size of the clusters on which reaction occurs, on their shape, and on their number, but also on the local density of the

reaction species. When the density is constant small clusters seem to dominate the behavior of the system at small p. The above factors have influenced the equivalent second-order reaction rate constants accordingly.

ACKNOWLEDGMENTS

One of us (P.L.) acknowledges financial aid from the Greek General Secretariat of Research and Technology.

[1]P. Lianos and S. Modes, J. Phys. Chem. **91**, 6088 (1987).
[2]P. Lianos, J. Chem. Phys. **89**, 5237 (1988).
[3]G. Duportail and P. Lianos, Chem. Phys. Lett. **149**, 73 (1988).
[4]A. Takami and N. Mataga, J. Phys. Chem. **91**, 618 (1987).
[5]A. Blumen, Nuovo Cimento **63B**, 50 (1981).
[6]J. Klafter and A. Blumen, J. Chem. Phys. **80**, 875 (1984).
[7]R. Kopelman, J. Stat. Phys. **42**, 185 (1986); J. Prasad and R. Kopelman, J. Phys. Chem. **91**, 265 (1987); Phys. Rev. Lett. **59**, 2103 (1987); D. Toussaint and F. Wilczek, J. Chem. Phys. **78**, 2642 (1983); K. Kang and S. Redner, Phys. Rev. Lett. **52**, 955 (1984).
[8]J. Lang, A. Jada, and A. Malliaris, J. Phys. Chem. **92**, 1946 (1988); see also references therein.
[9]P. Argyrakis and R. Kopelman, J. Phys. Chem. **91**, 2699 (1987); **93**, 225 (1989).
[10]P. Lianos, M. L. Viriot, and R. Zana, J. Phys. Chem. **88**, 1098 (1984).
[11]J. Klafter, A. Blumen, and G. Zumofen, J. Luminesc. **31/32**, 627 (1984).
[12]J. Hoshen, R. Kopelman, and E. M. Monberg, J. Stat. Phys. **19**, 219 (1978).
[13]S. Alexander and R. Orbach, J. Phys. Lett. **43**, L625 (1982).
[14]S. Havlin and D. ben-Avraham, Adv. Phys. **36**, 695 (1987).
[15]P. Meakin and H. E. Stanley, J. Phys. A **17**, L173 (1984).
[16]S. Modes and P. Lianos, J. Phys. Chem. (unpublished).